Projective filtering of the fundamental eigenmode from spatially multimode radiation

A. M. Pérez,[1,2,*] P. R. Sharapova,[3] S. S. Straupe,[3] F. M. Miatto,[4] O. V. Tikhonova,[3,5] G. Leuchs,[1,2] and M. V. Chekhova[1,2,3]

[1]*Max-Planck Institute for the Science of Light, Günther-Scharowsky-Str.1/Bau 24, Erlangen D-91058, Germany*

[2]*Institute of Optics, Information and Photonics, University of Erlangen-Nürnberg, Staudtstrasse 7/B2, 91058 Erlangen, Germany*

[3]*Physics Department, Moscow State University, Leninskiye Gory 1-2, Moscow 119991, Russia*

[4]*Department of Physics, University of Ottawa, Ottawa, ON, Canada K1N 6N5*

[5]*Skobeltsyn Institute of Nuclear Physics, Lomonosov Moscow State University, Moscow 119234, Russia*

(Received 23 February 2015; published 30 November 2015)

Lossless filtering of a single coherent (Schmidt) mode from spatially multimode radiation is a problem crucial for optics in general and for quantum optics in particular. It becomes especially important in the case of nonclassical light that is fragile to optical losses. An example is bright squeezed vacuum generated via high-gain parametric down conversion or four-wave mixing. Its highly multiphoton and multimode structure offers a huge increase in the information capacity provided that each mode can be addressed separately. However, the nonclassical signature of bright squeezed vacuum, photon-number correlations, are highly susceptible to losses. Here we demonstrate lossless filtering of a single spatial Schmidt mode by projecting the spatial spectrum of bright squeezed vacuum on the eigenmode of a single-mode fiber. Moreover, we show that the first Schmidt mode can be captured by simply maximizing the fiber-coupled intensity. Importantly, the projection operation does not affect the targeted mode and leaves it usable for further applications.

DOI: 10.1103/PhysRevA.92.053861 PACS number(s): 42.65.Lm, 42.50.Ar, 42.50.Dv, 42.65.Yj

I. INTRODUCTION

Sources with a perfectly single-mode spatial spectrum are desirable but rare; an example is a laser with the beam quality factor $M^2 = 1$. Most sources contain multiple spatial modes, which leads to the need for filtering methods. Preferably, these methods should be lossless; i.e., they should maintain all energy contained in the filtered mode. This is important for laser sources but becomes absolutely crucial for certain types of nonclassical light because of the destructive role of losses.

Although formally one can choose free-space modes in many different ways, the most common example being plane-wave modes, spatial coherence dictates a special choice of eigenmodes for each type of radiation. For instance, if a mode has to contain all spatially coherent radiation, it has to be chosen according to the Mercer expansion [1] of the first-order Glauber's correlation function. The Mercer expansion provides the so-called *coherent modes* because the radiation within each of them is coherent.

Very similar to Mercer expansion is the Schmidt decomposition. While the Mercer expansion describes coherence of partially coherent light, the Schmidt decomposition also accounts for photon-number correlations. Within a certain Schmidt mode the radiation is coherent and has photon-number correlations only with itself or with a single matching mode. Such modes, which typically are not monochromatic plane waves, have been used to describe nonclassical light, mostly for frequency or temporal modes and sometimes also for wave vector or spatial modes. Bennink and Boyd introduced the term "squeezing modes" for describing squeezing within a broad frequency spectrum of a traveling-wave parametric amplifier [2]. Opatrny and coworkers used the same concept to describe frequency correlations for Kerr-squeezed pulses in optical fibers [3]. It is worth stressing that the "squeezing modes" of Ref. [2] as well as the "broadband modes" of Ref. [3] and the Schmidt modes mentioned further here are the same eigenmodes, the ones that diagonalize the Hamiltonian producing the radiation. It has been shown [2] that without a proper selection of such modes, the degree of measured squeezing decreases considerably. This is a consequence of the fragility of squeezing to losses. In the case of multimode bright squeezed vacuum (BSV), generated through high-gain parametric down-conversion (PDC) [4] or four-wave mixing (FWM) [5], the necessity to filter out a single Schmidt mode in a clean way, without losing its photons or admixing photons from different modes, is especially important due to strong thermal fluctuations within each mode [6–8]. If unmatched modes are detected, these fluctuations completely destroy the squeezing.

There exists a partial solution in the case of homodyne detection, where one detects only the modes matching the ones of the local oscillator. It is therefore possible to select proper modes by tailoring the radiation of the local oscillator. In a series of works [9], Fabre, Treps, and coworkers studied BSV generated by frequency combs and its eigenmodes (referred to there as "supermodes"). They detected the eigenmodes selectively using a specially tailored local oscillator. A similar strategy of tailoring the local oscillator is applied in experiments with spatially multimode BSV produced via FWM [10]. However, in homodyne detection one cannot make use of the radiation in the selected mode, for instance, by coupling it with atoms or mechanical systems. If we seek any further use of nonclassical light, we need another type of projective filtering, a nondestructive one.

As a solution, here we consider filtering of a spatial mode with an optical fiber. We will show in Sec. II that an optical fiber performs the projection of the input spatial spectrum on its eigenmode, which can be considered, to a good approximation, as a Gaussian beam. We should stress that only in the case where the fiber eigenmode coincides with the radiation Schmidt mode, the filtering procedure will retain all features of the initial radiation such as coherence,

*Corresponding author: angela.perez@mpl.mpg.de

peculiarities of the photon statistics, nonclassicality, etc. We test the quality of such filtering by measuring the fraction of intensity transmitted through the fiber and comparing it with the theoretical expectation, which is the weight of the strongest mode in the Schmidt decomposition. As the radiation to be tested, we choose multimode BSV generated through high-gain PDC.

The goal of this work is to test the quality of filtering of a single coherent mode of PDC with an optical fiber. Many authors aimed at maximizing the total efficiency of coupling low-gain PDC (SPDC) radiation into an optical fiber [11]. It has been shown that the optimal case is the one of a rather tightly focused pump, when SPDC contains a few, almost a single, mode; but even under this condition the maximum coupling efficiency does not exceed 75% [11]. Besides, as we will show further, in this case the coupling of a single eigenmode is lossy. Other authors [12–14] maximize the heralding efficiency of signal and idler SPDC photons coupled into single-mode fibers. It was found that the heralding efficiency is maximal and nearly 100% for a softly focused pump and, correspondingly, for spatially multimode SPDC [13]. Here, in contrast, we consider the losses within a single eigenmode. In order to determine the shapes and weights of the eigenmodes for PDC radiation, we apply the Schmidt decomposition, which is considered in Sec. III. We describe the experiment in Sec. IV where we assess the quality of the filtering.

In the experiment, we deal with spatial (near-field) and angular (far-field) modes. Being parts of Fourier-conjugate spectra, they are alternative ways to describe the radiation. In Sec. V we consider the analogy of projective filtering for temporal or frequency spectra and propose a method for linear projective filtering of these modes. Finally, in Sec. VI we summarize the results.

II. PROJECTIVE FILTERING AND SPATIAL RADIATION EIGENMODES

A. Filtering with an aperture

If one needs to select a single mode from the angular (spatial) spectrum, the simplest strategy is to put an aperture of a certain size into the far (near) field. For a very small aperture, the mode selected this way will be a plane wave in the first case and a spherical wave in the second one. It is well known that the radiation after such filtering will be coherent (see, for instance, Ref. [1]). As a consequence, the statistical properties (such as photon-number distribution) of certain radiation types will be also maintained. This will be the case, for instance, for thermal light [1]. However, for more fragile types of light, e.g., squeezed vacuum, photon-number correlations will be lost [6,7]. Moreover, even if the aperture has a specially chosen size and intensity transmission repeating the intensity distribution of a single mode, the filtering will still be lossy.

B. Single-mode fiber as a projective filter

In order to maintain photon-number correlations, we require a different strategy, one in which only a single eigenmode is filtered out, or a pair of conjugated eigenmodes, in the case of light with bipartite correlations. It is important for the filtering

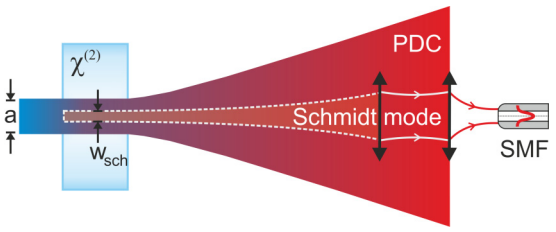

FIG. 1. (Color online) Filtering a single eigenmode of broadband PDC radiation with a single-mode fiber. W_{sch} is the width of the first Schmidt mode in the near field, a is the pump width.

to be of projective type: a single field mode of the incident radiation should be projected on the eigenmode of the filtering device. This kind of filtering is provided by a single-mode fiber [15], with the restriction that its eigenmode is a Bessel function, very close to a Gaussian. If a mode of any other shape has to be filtered, the fiber could be preceded by a spatial light modulator (SLM) performing the transformation from this shape to a Gaussian [15,16]. The only losses introduced this way will be the ones associated with the SLM or any alternative device.

As mentioned before, here we consider PDC as a source of multimode radiation (Fig. 1). The PDC radiation created in a nonlinear crystal has its near-field effective diameter related to the full width at half maximum (FWHM) a of the Gaussian pump. However, as it is multimode, its angular divergence is much larger than expected for a Gaussian beam of waist a. A single-mode fiber filters out the Gaussian Schmidt mode with the waist w_{sch} losslessly and blocks all other modes.

Mathematically the effect of the fiber is described as a projection operation. Let the eigenmode of the fiber in the near field be $f(\mathbf{r})$, $\int |f(\mathbf{r})|^2 d\mathbf{r} = 1$, with $\mathbf{r}$ being the coordinate at the input facet of the fiber, and the radiation eigenmodes be $u_n(\mathbf{r})$, $\int u_n^*(\mathbf{r}) u_k(\mathbf{r})\, d\mathbf{r} = \delta_{nk}$. Then we can write the photon annihilation operator $\hat{A}$ in the fiber mode as a linear combination of the photon annihilation operators $\hat{A}_k$ acting in the radiation eigenmodes, which form an orthonormal set:

$$\hat{A} = \sum_k C_k \hat{A}_k. \tag{1}$$

Here

$$C_k \equiv \int f(\mathbf{r}) u_k^*(\mathbf{r}) d\mathbf{r}, \quad \sum_k |C_k|^2 = 1 \tag{2}$$

are the projections of the fiber mode on the radiation eigenmodes. If a single radiation eigenmode $u_0(\mathbf{r})$ coincides with the fiber mode, its projection $C_0 = 1$ and the other projections are zero.

Equivalently, the modes can be described in the far field as $u_k(\mathbf{q})$, by introducing the transverse wave vector $\mathbf{q}$. Note that the same relation (1) will be valid for classical fields instead of the annihilation operators.

Relation (1) is the same as the one describing the field or operator at one output of a series of beam splitters in terms of the fields (operators) at their inputs (Fig. 2):

$$a_{\text{out}} = \sum_{k=0}^{n} C_k a_k, \quad \sum_{k=0}^{n} |C_k|^2 = 1. \tag{3}$$

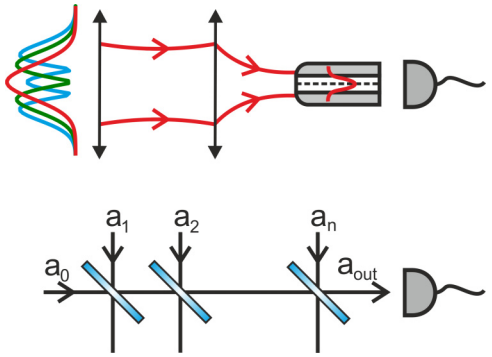

FIG. 2. (Color online) Analogy between multiple orthogonal modes projected on the eigenmode of a fiber and multiple input modes of several beam splitters projected on a single output mode.

The projections C_k depend then on the field transmission or reflection coefficients t_k, r_k :

$$C_0 = t_1 t_2 \ldots t_n, \quad C_1 = r_1 t_2 \ldots t_n, \ldots, \quad C_n = r_n. \tag{4}$$

C. Spatial radiation modes

In the classical case, the eigenmodes of free-space radiation are given by the Mercer expansion, defined through the first-order Glauber's correlation function $G^{(1)}(\mathbf{r}_1,\mathbf{r}_2)$ [1,17]:

$$G^{(1)}(\mathbf{r}_1,\mathbf{r}_2) = \sum_n \alpha_n u_n^*(\mathbf{r}_1) u_n(\mathbf{r}_2). \tag{5}$$

The modes $u_n(\mathbf{r})$ are called coherent modes because the radiation within each such a mode is coherent.

Whenever photon correlations between two beams are of interest, especially nonclassical photon-number correlations, rather than coherence within a single beam, Mercer decomposition is not sufficient and the Schmidt decomposition should be used, as will be shown in the next section addressing high-gain PDC.

III. HIGH-GAIN PDC AND ITS EIGENMODES

High-gain PDC is a convenient way to produce bright squeezed vacuum, a macroscopic quantum state of light that is among the most promising sources for quantum technologies. It manifests polarization and photon-number entanglement [18,19] and can violate Bell's inequality under certain experimental conditions [20]. It already has found applications in quantum imaging [21] and quantum metrology [22], in particular enabling phase supersensitivity [23]. BSV is multimode in angle and frequency and can have the mean photon number per mode as high as 10^{13} [24]. These features provide its high information capacity as quantum information can be encoded in the photon number of each mode. Ideally one would like to isolate and efficiently control each mode without losing its nonclassical correlations.

A. The Schmidt decomposition and the Bloch-Messiah reduction

The eigenmodes of BSV are found from the Schmidt decomposition, in which each mode of the signal beam is correlated to a single idler mode [15,25–29]. In signal and idler channels taken separately, the modes found this way coincide with the coherent modes from the Mercer expansion (5) [17,30].

It has been shown [29] that BSV exhibits the same Schmidt modes as two-photon light generated via low-gain PDC under the same experimental geometry. The modes are found by diagonalizing the Hamiltonian of PDC,

$$\hat{H} = i\hbar\Gamma \int d\mathbf{q}_s d\mathbf{q}_i F(\mathbf{q}_s,\mathbf{q}_i) \hat{a}^\dagger_{\mathbf{q}_s} \hat{a}^\dagger_{\mathbf{q}_i} + \text{H.c.}, \tag{6}$$

where Γ is the coupling parameter scaling as the pump amplitude, $\mathbf{q}_s, \mathbf{q}_i$ the signal and idler transverse wave vector components, $\hat{a}^\dagger_{\mathbf{q}_s} \hat{a}^\dagger_{\mathbf{q}_i}$ the photon creation operators in the corresponding plane-wave modes, and $F(\mathbf{q}_s,\mathbf{q}_i)$ the two-photon amplitude (TPA). This term, as it is used here, is conventional: at strong pumping, photons are no more emitted in pairs but in large even numbers. The Hamiltonian is diagonalized through the Schmidt decomposition of the TPA,

$$F(\mathbf{q}_s,\mathbf{q}_i) = \sum_{m,n} \sqrt{\lambda_{mn}} u_{mn}(\mathbf{q}_s) v_{mn}(\mathbf{q}_i), \tag{7}$$

where λ_{mn} are the Schmidt eigenvalues, $\sum_{m,n} \lambda_{mn} = 1$, and $u_{mn}(\mathbf{q}_s), v_{mn}(\mathbf{q}_i)$ are the 2D Schmidt modes of the signal and idler radiation. In the degenerate case, where signal and idler beams are indistinguishable, $u_{mn}(\mathbf{q}) = v_{mn}(\mathbf{q})$.

After substituting Eq. (7) into Eq. (6), the Hamiltonian can be written in the diagonal form (the Bloch-Messiah reduction) [29],

$$H = i\hbar\Gamma \sum_k \sqrt{\lambda_k} (\hat{A}^\dagger_k \hat{B}^\dagger_k - \hat{A}_k \hat{B}_k), \tag{8}$$

where $k \equiv \{m,n\}$ and $\hat{A}^\dagger_k, \hat{B}^\dagger_k$ are photon creation operators for the Schmidt modes defined as

$$\hat{A}^\dagger_k = \int d\mathbf{q}_s u_k(\mathbf{q}_s) a^\dagger_{\mathbf{q}_s}, \quad \hat{B}^\dagger_k = \int d\mathbf{q}_i v_k(\mathbf{q}_i) a^\dagger_{\mathbf{q}_i}. \tag{9}$$

In order to label the photons as signal or idler, we assume here some additional degree of freedom, for instance, different wavelengths as in nondegenerate PDC. The solution to the Heisenberg equations for the operators in Schmidt modes leads to Bogolyubov-type transformations between the input operators $\hat{A}_{k0}, \hat{B}_{k0}$ and the output ones $\hat{A}_k, \hat{B}_k$ [29],

$$\begin{aligned} \hat{A}_k &= c_k \hat{A}_{k0} + s_k \hat{B}^\dagger_{k0}, \\ \hat{B}_k &= c_k \hat{B}_{k0} + s_k \hat{A}^\dagger_{k0}, \end{aligned} \tag{10}$$

where

$$c_k = \cosh(G\sqrt{\lambda_k}), \quad s_k = \sinh(G\sqrt{\lambda_k}), \tag{11}$$

and $G = \int \Gamma\, dt$ is the parametric gain.

The mean photon number in mode k is $N_k = s_k^2$, and the total mean photon number in each (signal or idler) beam is given by the incoherent sum over separate Schmidt modes: $N = \sum_k s_k^2$. Thus, the Schmidt eigenvalues at high gain are renormalized [29],

$$\lambda'_k = \frac{s_k^2}{N} = \frac{\sinh^2(G\sqrt{\lambda_k})}{\sum_k \sinh^2(G\sqrt{\lambda_k})}, \tag{12}$$

so that the eigenvalue λ'_k of a certain Schmidt mode determines the contribution of this mode to the total number of photons,

$N_k = N\lambda'_k$. The effective number of Schmidt modes, in the low-gain regime given by the Schmidt number $K = [\sum_k \lambda_k^2]^{-1}$, is hence reduced at high gain, $K' = [\sum_k \lambda_k'^2]^{-1}$.

The signal photon annihilation operator $\hat{A}$ after the fiber is then given by Eq. (1), with $\hat{A}_k$ being the photon annihilation operators in the signal Schmidt modes and the projections C_k given by Eq. (2). A similar expression is valid for the idler photon annihilation operator $\hat{B}$ after the fiber: $\hat{B} = \sum_k D_k \hat{B}_k$, with D_k denoting the projections of the idler Schmidt modes on the fiber eigenmode. We assume here that the fiber mode function is identical for the signal and idler photons. The mean photon numbers after the fiber are

$$\begin{aligned} N_s &= \langle \hat{A}^\dagger \hat{A} \rangle = \sum_k |C_k|^2 s_k^2 = N \sum_k |C_k|^2 \lambda'_k, \\ N_i &= \langle \hat{B}^\dagger \hat{B} \rangle = \sum_k |D_k|^2 s_k^2 = N \sum_k |D_k|^2 \lambda'_k. \end{aligned} \tag{13}$$

B. The two-crystal scheme

In our experiment, described further in Sec. IV, PDC is generated in two consecutive nonlinear crystals placed into a common Gaussian pump beam. For two crystals of length L at a distance l, the normalized TPA for frequency-degenerate or nearly degenerate type-I PDC has the form [29,31]

$$\begin{aligned} F(\mathbf{q}_s, \mathbf{q}_i) = \exp\left[-\frac{a^2 k_0^2}{8 \ln 2} \left\{ \left(\theta_s^2 + \theta_i^2\right) + 2\theta_s \theta_i \cos(\phi_s - \phi_i) \right\} \right] \\ \times \operatorname{sinc}\left(\frac{\Delta k_z L}{2} \right) \cos\left(\frac{\Delta k_z L + \Delta k'_z l}{2} \right) \\ \times \exp(-i\,\Delta k_z L) \exp\left(\frac{-i\,\Delta k'_z l}{2} \right), \end{aligned} \tag{14}$$

where k_0 is the length of signal and idler wave vectors, $\theta_{s,i}, \phi_{s,i}$ are their spherical angles, a is the full width at half maximum (FWHM) of the pump intensity distribution, $\Delta k_z = k_p - k_0[\cos(\theta_s) + \cos(\theta_i)]$ is the longitudinal mismatch inside each crystal, and k_p is the length of the pump wave vector. In its turn, $\Delta k'_z = k_p^{\text{air}} - k_0^{\text{air}}[\cos(\Theta_s) + \cos(\Theta_i)]$ is the longitudinal mismatch in the air gap between the crystals, where the pump and signal or idler wave vectors take values k_p^{air} and k_0^{air}, respectively; $\Theta_{s,i} = \frac{n_0}{n_0^{\text{air}}}\theta_{s,i}$, and n_0, n_0^{air} are the signal or idler refractive indices inside the crystals and inside the air gap, respectively.

The Schmidt decomposition is most conveniently found in the cylindrical frame of reference, in which the transverse wave vectors $\mathbf{q}_{s,i}$ are given by their modules, $q_{s,i} = k_0 \sin\theta_{s,i}$, and the azimuthal angles, $\phi_{s,i}$ [16,30]. In this case, $F(\mathbf{q}_s, \mathbf{q}_i)$ can be written as a Fourier expansion due to its periodicity in $(\phi_s - \phi_i)$ [16],

$$F(q_s, q_i, \phi_s - \phi_i) = \sum_n \chi_n(q_s, q_i) e^{in(\phi_s - \phi_i)}, \tag{15}$$

where $\chi_n(q_s, q_i)$ can be found using the inverse Fourier transformation. Then the Schmidt decomposition of $\chi_n(q_s, q_i)$ yields

$$\chi_n(q_s, q_i) = \sum_m \sqrt{\lambda_{mn}} \frac{\tilde{u}_{mn}(q_s)}{\sqrt{q_s}} \frac{\tilde{v}_{mn}(q_i)}{\sqrt{q_i}} \tag{16}$$

with the functions $\tilde{u}_{mn}(q_s)$ and $\tilde{v}_{mn}(q_i)$ obeying the normalization condition

$$\int_0^\infty dq_s \tilde{u}_{mn}(q_s) \tilde{u}^*_{kn}(q_s) = \int_0^\infty dq_i\, \tilde{v}_{mn}(q_i) \tilde{v}^*_{kn}(q_i) = \delta_{mk}.$$

From Eq. (16), we obtain the Schmidt decomposition of the TPA (7) with $u_{mn}(\mathbf{q}_s) = \frac{\tilde{u}_{mn}(q_s)}{\sqrt{q_s}} e^{in\phi_s}, v_{mn}(\mathbf{q}_i) = \frac{\tilde{v}_{mn}(q_i)}{\sqrt{q_i}} e^{-in\phi_i}$.

C. Filtering the first Schmidt mode

The first Schmidt mode u_{00} of the BSV state, a Gaussian of waist w_{sch}, can be filtered by projecting the angular spectrum on the eigenmode of a fiber, which is close to a Gaussian of waist w, $f(\mathbf{q}) = (\sqrt{\pi} w)^{-1} \exp(-q^2/2w^2)$. The projections of different Schmidt modes on the eigenmode of the fiber are [see Eq. (2)]

$$C_{mn} = \int_0^{2\pi} d\phi \int_0^\infty q\, dq\, f(q,\phi) u_{mn}(q,\phi), \tag{17}$$

$\sum_{m,n} |C_{mn}|^2 = 1$. Note that since the fiber mode does not depend on ϕ, only Schmidt modes with $n = 0$ will contribute in the coupling efficiency.

From (13), the coupling efficiency T for the signal radiation is obtained by summing the photon numbers that couple into the fiber from different modes:

$$T = \sum_{m,n} |C_{mn}|^2 \lambda'_{mn} \leqslant \lambda'_{00}. \tag{18}$$

The last inequality follows from the fact that $\lambda'_{m\geqslant 0, n\geqslant 0} \leqslant \lambda'_{00}$ and shows that the photon number transmitted through the fiber is maximized when the fiber mode exactly matches the first Schmidt mode, $|C_{00}| = 1$, and $T_{\max} = \lambda'_{00}$. In this case the first Schmidt mode is filtered perfectly, without losses. Only in this case the filtered Schmidt mode maintains all specific features of the incoming PDC radiation including nonclassicality.

D. The absence of losses

However, for the first Schmidt mode to coincide with the fiber eigenmode, the former should be real or at least have no spatially varying phase, as the latter is a real Gaussian function. At the same time, Eq. (14) for the TPA includes some phase factors; moreover, even the TPA for a single crystal is complex [29]. As a consequence the Schmidt modes of down-converted radiation can be complex functions. In this case the projection amplitudes C_{mn} entering Eq. (18) are reduced. Using the Cauchy-Schwarz inequality one can show that the maximal projection amplitude for the first Schmidt mode $u_{00}(q,\phi)$ and the fiber eigenmode $f(q,\phi)$ will be still less than 1 if the Schmidt mode is complex. Indeed,

$$\begin{aligned} |C_{00}|^2 \leqslant \int_0^{2\pi} d\phi \int_0^\infty q\, dq |f(q,\phi)|^2 \\ \times \int_0^{2\pi} d\phi \int_0^\infty q\, dq |u_{00}(q,\phi)|^2 = 1, \end{aligned} \tag{19}$$

with the equality valid only in the case where the Schmidt mode and the fiber eigenmode coincide up to a constant phase factor. Whenever $|C_{00}| < 1$, the filtering procedure leads to intrinsic losses. Now let us consider under what circumstances the first Schmidt mode would be strongly complex. The TPA (14) is

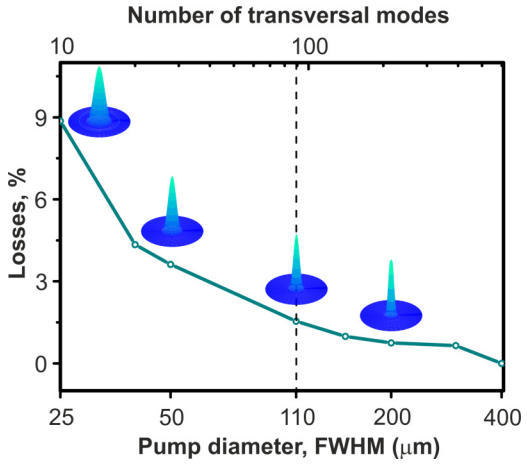

FIG. 3. (Color online) Numerical estimation of losses accompanying the filtering of PDC generated in the two-crystal system. The pump diameter a is varied in order to change the initial number K of the transversal modes. The dashed line corresponds to the parameters used in our experiment. The insets show the intensity distributions of the first Schmidt mode for various points in the transverse-wave vector space.

complex due to the phase factor $\exp\{-i\Delta k_z L - i\Delta k_z' l/2\}$, which does not depend on the pump beam waist a. At the same time, the size of the first Schmidt mode does depend on a. By choosing appropriate a, one can find the conditions under which the phase of the TPA does not vary noticeably within the scale of the first Schmidt mode. In this case, the left part of (19) will be close to 1 and the losses will be negligibly small.

To demonstrate this, we have performed the Schmidt decomposition and calculated C_{00} for various diameters a of the pump. For each case, the shape of the first Schmidt mode was calculated (the corresponding intensity distributions in transverse wave vector space are shown as insets in Fig. 3). Further, the losses accompanying the filtering, given by $1 - |C_{00}|^2$, were numerically calculated (shown in Fig. 3 as points connected by a line.) The result is that the weaker the focusing, the smaller the losses. From the inset, one can also notice that for weaker focusing, the first Schmidt mode is narrower and this is why the TPA phase in its vicinity is flat. For focusing into more than 100 μm, the losses are less than 1.5%. In our experiment, we use $a = 110\,\mu$m, which corresponds to 2% of losses (shown in Fig. 3 by dashed line).

Thus, for a weakly focused pump, the first Schmidt mode has a flat phase and can be filtered nearly losslessly using a single-mode fiber. In the opposite case of a tightly focused pump, projective filtering with a single-mode fiber is lossy. In principle, even in this case, the phase of the Schmidt mode to be filtered can be eliminated before coupling the light into the fiber, but this requires some special efforts like using an SLM.

Note that experiments with SPDC report high (up to 96%) heralding efficiencies with a softly focused pump [13,14], despite a low generation rate of photons. This is in agreement with our observation (Fig. 3): if the heralded mode coincides with the Schmidt mode of a highly multimode state, the losses of its fiber coupling can be indeed negligible. In contrast, with the pump tightly focused into the crystal, so that the resulting

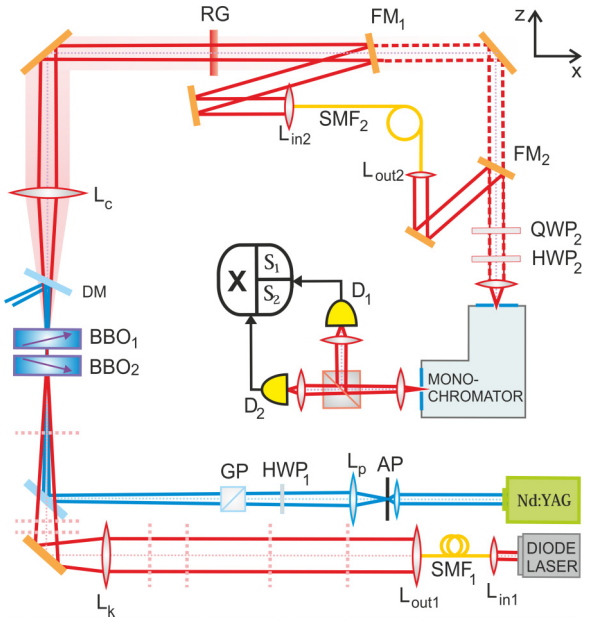

FIG. 4. (Color online) Setup scheme. The third harmonic of a Nd:YAG laser, mode cleaned and properly polarized (aperture AP, half-wave plate HWP_1 and Glan prism GP), focused into crystals BBO_1 and BBO_2 by lens L_p, generates PDC. An auxiliary laser diode beam, mode cleaned by a single-mode fiber SMF_1, serves to emulate the spatial distribution of different Gaussian modes, with the waists in the same plane. These modes are prepared with the help of different lenses L_k, placed at the planes marked by the vertical dotted lines one at a time. A Gaussian mode is filtered by the single-mode fiber SMF_2 after lenses L_c, L_{in2}. Flipping mirrors FM_1 and FM_2 separate the filtering path from the free-space path (dashed lines). Before PDC enters the monochromator, its polarization is adjusted by half-wave and quarter-wave plates (HWP_2, QWP_2). Finally, the signals are analyzed in a Hanbury Brown-Twiss interferometer including detectors D_1 and D_2.

number of modes is small [11], the coupling efficiency is never high, again in agreement with our calculations (Fig. 3). At the same time, the efficiency of filtering a single mode has been never directly measured before. The next section considers this measurement.

IV. EXPERIMENT

A. Intensity measurements

The BSV state is generated via high-gain PDC (Fig. 4) in two 1 mm long beta barium borate crystals (BBO_1, BBO_2) cut for type-I collinear degenerate phase matching and arranged in the anisotropy compensating configuration at the closest achievable distance of 2.5 ± 0.5 mm [32–34]. The crystals are pumped by a Nd:YAG laser third harmonic (wavelength 355 nm, pulse duration 18 ps, and repetition rate 1 kHz). The pump is mode-cleaned by means of a diamond pinhole (AP) and its polarization is set by a Glan prism (GP) and a half-wave plate HWP_1. The pump waist is imaged by lens L_p (100 mm focal length) onto the plane between the crystals, where its FWHM is 110 um $\pm$ 5 um. This experimental configuration in the low-gain regime creates a two-photon state with the spatial Schmidt number $K = 89$ [Fig. 5(a)]. The first Schmidt mode

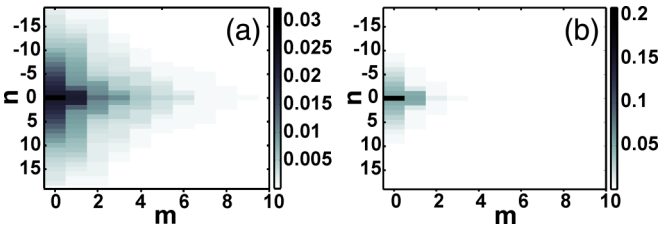

FIG. 5. (Color online) The Schmidt eigenvalues for PDC from the two-crystal scheme used in our experiment (a) in the low-gain regime, resulting in the effective mode number $K = 89$, and (b) in the high-gain regime, resulting in $K' = 14.7$.

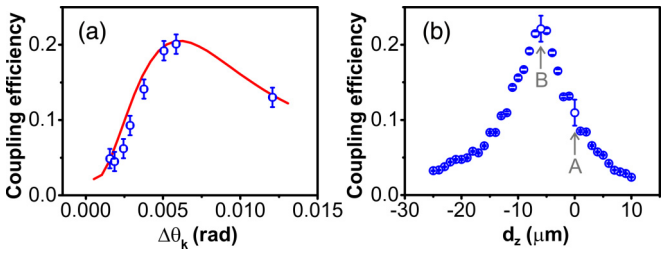

FIG. 6. (Color online) Spatial filtering of PDC radiation: the coupling efficiency (a) versus the angular width $\Delta\theta_k$ of the Gaussian beam coupled into the fiber and (b) versus the longitudinal adjustment d_z of the coupling system. The bars at points A and B show the absolute uncertainty of the coupling efficiency.

is very close to a Gaussian function, with the divergence 0.006 rad and the waist 53 μm. Our experiment is performed in the high-gain regime (pump power 70 mW), which, according to Eq. (12), leads to the reduction in the number of spatial modes. The resulting Schmidt number is calculated to be $K' = 14.7$ [Fig. 5(b)] for $G = 22.8$.

After the crystals, the pump radiation is cut off by a dichroic mirror (DM) and a red glass filter RG 650 (RG). The spatial filtering is performed by a standard step index single-mode fiber (SMF_2, Thorlabs SM600). In the experiment we filter from the PDC radiation, with the help of the fiber, Gaussian beams with different waists or divergences and measure the fraction T of PDC intensity transmitted through the fiber. According to Eq. (18), the largest T should equal the first Schmidt eigenvalue and should be achieved when the coupled Gaussian mode coincides with the first Schmidt mode.

For emulating Gaussian beams with various waists, we use an additional CW diode laser with the wavelength 706.5 nm. The diode laser beam is mode-cleaned by a single-mode fiber SMF_1, collimated by lens L_{out1}, and then overlapped with the pump beam on the crystals after passing through one of the lenses L_k, with the other lenses removed from the beam. Each lens is aligned so that it forms the beam waist of a certain diameter w_k (measured by a beam profiler) on the crystals. For each waist diameter, the beam is coupled into SMF_2 by means of lens L_c (150 mm focal length) and aspheric lens L_{in2} (3.3 mm focal length), with the losses 12%–18% including 4% reflection at the uncoated input facet. For each lens L_k, efficient coupling of the diode laser beam into the fiber indicates that the system filters out a Gaussian mode with a certain waist w_k and the corresponding divergence $\Delta\theta_k$. After this, the diode laser is switched off and the spatial filtering is applied to the PDC radiation. Light out-coupled from the fiber is sent through a monochromator selecting a bandwidth of 0.1 nm around the nondegenerate wavelength 708 nm. Zero-order quarter-wave plate (QWP_2) and half-wave plate (HWP_2) optimize the incoming polarization on the monochromator and minimize losses.

For comparing the data in the presence and in the absence of filtering, a free-space channel is used where the PDC radiation is sent to the monochromator directly, avoiding the fiber (Fig. 4). Switching between the free-space and spatially filtered channels is done with the flipping mirrors FM1 and FM2. The efficiency T of coupling into the fiber is measured by dividing the sum signal of the detectors D_1 and D_2 in the presence of filtering by the one in its absence.

Since each Gaussian beam is coupled to SMF_2 with $85\% \pm 3\%$ coupling efficiency, the PDC coupling is underestimated. We quantify these technical losses and correct for them at each measured point. In the free-space configuration we also measure the total number of spatial modes through the normalized second-order intensity correlation function $g^{(2)}$ at the nondegenerate wavelength of 708 nm, making sure that all angular spectrum is collected. Then the measured correlation function depends on the number of modes K' as $g^{(2)} = 1 + 1/K'$ [34]. We obtain $g^{(2)} = 1.07 \pm 0.01$, which indicates $K' = 15 \pm 2$ spatial modes, in agreement with the calculation [Fig. 5(b)].

Figure 6(a) shows the coupling efficiencies for each angular width $\Delta\theta_k$ of the filtered Gaussian mode as well as the theoretical curve, with a good agreement between the two. Both curves have their maximum at an angular width of 6 mrad, which is the angular divergence of the first Schmidt mode. Moreover, the maximum coupling efficiency achieved experimentally is 0.201 ± 0.005, which matches the first Schmidt eigenvalue $\lambda'_{00} = 0.205$ calculated for our BSV state (Fig. 5). From these values, the losses of the filtering procedure do not exceed 2%, as expected from the calculation (Fig. 3). This proves that filtering of the first Schmidt mode of PDC radiation with a single-mode fiber is nearly lossless, up to reflections at the fiber facets and imperfect coupling.

Thus, the efficiency of coupling PDC radiation into the fiber is maximal when the first Schmidt mode coincides with the fiber eigenmode. One can guess that the first Schmidt mode can be targeted by simply maximizing the coupling efficiency. In what follows, we show that this is indeed the case. In fact, this is the strategy usually applied for low-gain PDC [11], but up to now it has not been tested for the filtering of a single mode.

Starting from a setting where a "wrong" Gaussian mode is coupled into the fiber [first point from the right in Fig. 6(a) and point A in Fig. 6(b)], we improve the PDC coupling by varying the distance between lens L_{in2} and the tip of the fiber. This way, we are able to achieve the coupling efficiency equal to the first Schmidt eigenvalue [point B in Fig. 6(b)]. This indicates that the mode collected is indeed the targeted Schmidt mode. Note that we achieve this goal by simply moving the fiber tip. At first sight impossible, it is feasible in our scheme due to the fact that in Gaussian optics, the position of the waist image depends on the initial waist size. As a result, modification of the beam waist on the crystals mainly leads to the displacement

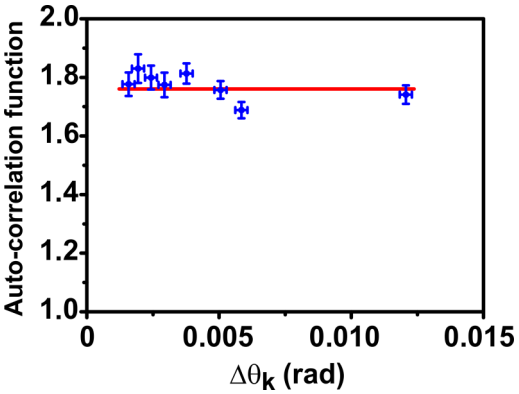

FIG. 7. (Color online) $g^{(2)}_{ss}$ measurement at the nondegenerate wavelength $\lambda_{\text{ndeg}} = 708$ nm versus the angular width of the Gaussian mode coupled into the fiber.

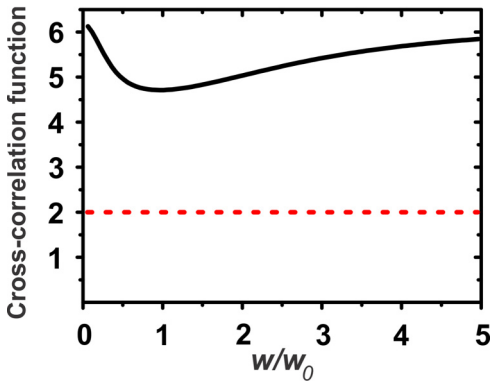

FIG. 8. (Color online) Dependence of the cross-correlation function $g^{(2)}_{si}$ on the size of the mode coupled into the fiber for two values of the gain: $G = 1$ (black continuous line) and $G = 10$ (red dashed line). The width is given in relative units w/w_0, where w_0 is the width of the (approximately) Gaussian first Schmidt mode. In both cases the Schmidt number $K' = 5$.

of the beam waist after lens L_{in2} rather than to the change of its size.

B. Correlation measurements

One might think that the mode filtering quality could be controlled by means of the correlation function measurement [27,28,34] since it usually indicates the number of modes. However, the measured autocorrelation function of the signal radiation at zero time delay, $g^{(2)}_{ss}(0)$ (further, simply $g^{(2)}_{ss}$, Fig. 7), is independent of the angular width of the Gaussian mode fully coupled into the fiber, and hence of the number of Schmidt modes contributing to the fiber output.

This can be understood from the analogy with a multiport beam splitter (Fig. 2). Indeed, with the thermal light at the input ports of a beam splitter, the statistics of light at each of its output ports will be also thermal [35,36]. Since each mode of PDC radiation has thermal statistics, the radiation at the output of the fiber will be thermal, and one will measure $g^{(2)}_{ss} = 2$ regardless of the number of modes contributing. Since our frequency filtering is not perfect, the measured value is lower, $g^{(2)}_{ss} = 1.76 \pm 0.02$, as shown in Fig. 7.

This shows that the quality of filtering cannot be assessed from the correlation function measurement for thermally populated Schmidt modes. At the same time, if the modes are populated with two-photon light, correlation measurements will indicate whether one or several modes are contributing to the fiber output.

Indeed, consider the normalized second-order correlation function at zero time delay after the spatial mode filter, the *autocorrelation function*

$$g^{(2)}_{ss} = \frac{\langle A^\dagger A^\dagger A A\rangle}{N_s^2} = \frac{1}{N_s^2}\sum_{i,j,k,l}(C_i)^*(C_j)^* C_k C_l \langle A_i^\dagger A_j^\dagger A_k A_l\rangle, \tag{20}$$

and the *cross-correlation function*

$$g^{(2)}_{si} = \frac{\langle A^\dagger B^\dagger A B\rangle}{N_s N_i} = \frac{1}{N_s N_i}\sum_{i,j,k,l}(C_i)^*(D_j)^* C_k D_l \langle A_i^\dagger B_j^\dagger A_k B_l\rangle. \tag{21}$$

A straightforward calculation using (10) gives

$$\begin{aligned}\langle A_i^\dagger A_j^\dagger A_k A_l\rangle &= s_i s_j s_k s_l(\delta_{jk}\delta_{il} + \delta_{ik}\delta_{jl}),\\ \langle A_i^\dagger B_j^\dagger A_k B_l\rangle &= s_i c_j c_k s_l \delta_{ij}\delta_{kl} + s_i s_j s_k s_l \delta_{ik}\delta_{jl}.\end{aligned} \tag{22}$$

Substituting (22) into (20) and (21) we get the following expressions for the second-order correlation functions:

$$\begin{aligned} g^{(2)}_{ss} &\equiv 2,\\ g^{(2)}_{si} &= 1 + \frac{\left|\sum_i C_i^* D_i^* s_i c_i\right|^2}{\left(\sum_i |C_i|^2 s_i^2\right)\left(\sum_k |D_k|^2 s_k^2\right)}.\end{aligned} \tag{23}$$

The autocorrelation function is identically equal to 2, in accordance with the multiport analogy and the results of our measurement (Fig 7). The behavior of the cross-correlation function is more subtle. Its value depends on both coupling coefficients between the Schmidt modes and the fiber mode and the partial photon numbers in each Schmidt mode. In the simplest case where the fiber matches the first Schmidt mode, i.e., $|C_k| = |D_k| = \delta_{k0}$, the expression for $g^{(2)}_{si}$ simplifies to

$$g^{(2)}_{si} = 2 + \frac{1}{s_0^2} = 2 + \frac{1}{N_0}, \tag{24}$$

where N_0 is the mean photon number in the first Schmidt mode. In this case the correlation function after the mode filter correctly describes the statistics of a single mode of the initial PDC source. However, when the mode matching is not perfect and several modes have significantly nonzero coupling coefficients, the correlation function value deviates from the expression expected for a single-mode PDC field. The dependence on the fiber mode waist, calculated using the double-Gauss model for the TPA, is shown in Fig. 8. At first sight, it looks unusual that the normalized cross-correlation function is minimal for the case of optimal coupling. However, this is in line with the usual dependence of normalized cross-correlation function for PDC on the mean photon number, given by Eq. (24). At larger photon numbers, PDC always has lower normalized cross-correlation function. Therefore,

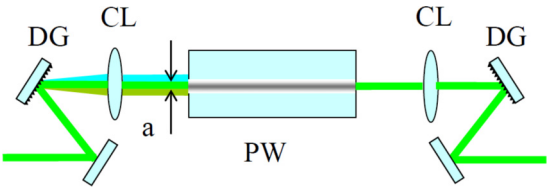

FIG. 9. (Color online) Setup for linear projective filtering of the frequency modes. DG, diffraction grating; CL, cylindrical lens, PW, planar waveguide; a, the size of its eigenmode.

optimal coupling, giving the maximal mean photon number, at the same time results in a minimum of the cross-correlation function. Unfortunately, the dependence flattens out with increasing gain, making the effect unobservable under current experimental conditions.

V. TEMPORAL OR FREQUENCY ANALOGY

A natural question arises whether a similar technique can be applied to filtering a single frequency mode from a multimode spectrum. There have been proposals of doing this by means of up-conversion, with the pump mode properly tailored in frequency [28,37]. A "quantum phase gate" based on this principle has been recently demonstrated to provide 80% efficiency for coherent pulses at the input [38]. This kind of filtering is also of projective type as it projects the field mode on the eigenmode of the converter. However, the method is technically complicated, requires phase matching within a broad frequency range, may have additional losses for external radiation fed into the nonlinear converter, and will be also influenced by noise whenever weak input radiation is considered (a feature of all similar up-converting devices).

By analogy with the spatial filtering introduced above, we can suggest a similar scheme for the filtering of the frequency or temporal modes, based on converting the frequency into the angle and then filtering the angle. The proposed setup (Fig. 9) is based on a 4f pulse shaper, in which the input multimode pulse falls on a diffraction grating followed by a cylindrical lens. In the focal plane of the lens the vertical coordinate scales linearly with the wavelength. In a usual 4f system, a spatially selective device such as a slit or an SLM is placed, after which another cylindrical lens and a diffraction grating collect the radiation into a single beam. To make the filtering projective, one can replace the spatial filter in the middle of the 4f scheme by a planar waveguide whose eigenmode has a Gaussian profile in the vertical direction. The size a of the mode should correspond to the frequency width of the Gaussian mode to be filtered. This device will project the frequency spectrum on a Gaussian one. If a more complicated frequency mode has to be filtered out, a mode converter (for instance, an SLM) should be placed before the planar waveguide.

VI. CONCLUSION

In this paper, we have considered the spatial filtering performed by a single-mode fiber and have shown that, in contrast to the filtering performed by an aperture, it is of projective type and therefore imposes no losses on the mode filtered out. An analogy between a fiber and a multiport beam splitter has been drawn. Based on this analogy, we have considered this type of filtering for the spatial modes of high-gain PDC. It was shown that only under the condition that the pump is focused into the crystal not too tightly, this filtering can be practically lossless. Otherwise, if the pump waist is small, the Schmidt modes have spatially nonuniform phases and the filtering will be lossy unless a phase correction is applied.

Further, we have demonstrated projective filtering of the first Schmidt mode from the spectrum of high-gain PDC in experiment. The total losses accompanying the filtering are only caused by imperfect alignment as well as the reflection on the uncoated fiber facet and do not exceed 15%. Importantly, the radiation in the mode filtered out this way is not destroyed and is available for further use. The method can be extended to higher-order spatial modes by using appropriate spatial-mode transformations, for instance, with the help of a spatial light modulator. Furthermore, it has been shown that the correct Schmidt mode can be filtered simply by maximizing the coupling into the fiber, provided that the apertures of the lenses do not clip significant portions of the radiation. The transmissivity of the fiber being close to the first Schmidt eigenvalue can be therefore used as a criterion for the selection of the first Schmidt mode. On the other hand, the autocorrelation function cannot be used for this purpose as it is independent on the number of modes contributing to the fiber output intensity. The cross-correlation function can be used to characterize the number of modes contributing but only at low parametric gain.

Finally, a similar technique has been proposed for the filtering of a single frequency mode out of the PDC spectrum. It is based on a standard 4f pulse-shaping scheme where a planar waveguide is used as a spatially selective element.

ACKNOWLEDGMENTS

The research leading to these results has received funding from the EU FP7 under Grant No. 308803 (project BRISQ2). We also acknowledge partial financial support of the Russian Foundation for Basic Research, Grants 14-02-31084 mol_-a and 14-02-00389_-a. P.R.Sh. acknowledges support of the "Dynasty" foundation.

[1] L. Mandel and E. Wolf, *Optical Coherence and Quantum Optics* (Cambridge University Press, Cambridge, 1995).

[2] R. S. Bennink and R. W. Boyd, Phys. Rev. A **66**, 053815 (2002).

[3] T. Opatrny, N. Korolkova, and G. Leuchs, Phys. Rev. A **66**, 053813 (2002).

[4] O. Jedrkiewicz, Y.-K. Jiang, E. Brambilla, A. Gatti, M. Bache, L. A. Lugiato, and P. Di Trapani, Phys. Rev. Lett. **93**, 243601 (2004); M. Bondani, A. Allevi, G. Zambra, M. G. A. Paris, and A. Andreoni, Phys. Rev. A **76**, 013833 (2007); G. Brida, L. Caspani, A. Gatti, M. Genovese, A. Meda, and I. R. Berchera,

Phys. Rev. Lett. **102**, 213602 (2009); T. Sh. Iskhakov, M. V. Chekhova, and G. Leuchs, *ibid.* **102**, 183602 (2009).

[5] V. Boyer, A. M. Marino, R. C. Pooser, and P. D. Lett, Science **321**, 544 (2008); V. Boyer, A. M. Marino, and P. D. Lett, Phys. Rev. Lett. **100**, 143601 (2008); N. Corzo, A. M. Marino, K. M. Jones, and P. D. Lett, Opt. Express **19**, 21358 (2011).

[6] P. P. Rohde, W. Mauerer, and C. Silberhorn, New J. Phys. **9**, 91 (2007).

[7] M. V. Chekhova and G. O. Rytikov, JETP **107**, 923 (2008).

[8] I. N. Agafonov, M. V. Chekhova, and G. Leuchs, Phys. Rev. A **82**, 011801 (2010).

[9] G. Patera, N. Treps, C. Fabre, and G. J. de Valcarcel, Eur. Phys. J. D **56**, 123 (2010); O. Pinel, P. Jian, R. M. de Araujo, J. Feng, B. Chalopin, C. Fabre, and N. Treps, Phys. Rev. Lett. **108**, 083601 (2012); J. Roslund, R. Medeiros de Araujo, Sh. Jiang, C. Fabre, and N. Treps, Nature Phot. **8**, 109 (2014).

[10] C. S. Embrey, M. T. Turnbull, P. G. Petrov, and V. Boyer, Phys. Rev. X **5**, 031004 (2015).

[11] C. Kurtsiefer, M. Oberparleiter, and H. Weinfurter, Phys. Rev. A **64**, 023802 (2001); F. A. Bovino, P. Varisco, A. M. Colla, G. Castagnoli, G. Di Giuseppe, and A. V. Sergienko, Optics Comm. **227**, 343 (2003); D. Ljunggren and M. Tengner, Phys. Rev. A **72**, 062301 (2005); W. P. Grice, R. S. Bennink, D. S. Goodman, and A. T. Ryan, *ibid.* **83**, 023810 (2011).

[12] J.-L. Smirr, M. Deconinck, R. Frey, I. Agha, E. Diamanti, and I. Zaquine, J. Opt. Soc. Am. B **30**, 288 (2013).

[13] P. B. Dixon, D. Rosenberg, V. Stelmakh, M. E. Grein, R. S. Bennink, E. A. Dauler, A. J. Kerman, R. J. Molnar, and F. N. C. Wong, Phys. Rev. A **90**, 043804 (2014).

[14] T. Guerreiro, A. Martin, B. Sanguinetti, N. Bruno, H. Zbinden, and R. T. Thew, Opt. Express **21**, 27641 (2013).

[15] S. S. Straupe, D. P. Ivanov, A. A. Kalinkin, I. B. Bobrov, and S. P Kulik, Phys. Rev. A **83**, 060302 (2011).

[16] F. M. Miatto, T. Brougham, and A. M. Yao, Eur. Phys. J. D **66**, 183 (2012).

[17] I. B. Bobrov, S. S. Straupe, E. V. Kovlakov, and S. P Kulik, New J. Phys. **15**, 073016 (2013).

[18] M. V. Chekhova, G. Leuchs, and M. Zukowski, Opt. Comm. **337**, 27 (2015).

[19] T. Sh. Iskhakov, I. N. Agafonov, M. V. Chekhova, and G. Leuchs, Phys. Rev. Lett. **109**, 150502 (2012).

[20] K. Rosolek, M. Stobinska, M. Wiesniak, and M. Zukowski, Phys. Rev. Lett. **114**, 100402 (2015).

[21] G. Brida, M. Genovese, and I. Ruo Berchera, Nature Photonics **4**, 227 (2010); A. Gatti, E. Brambilla, L. A. Lugiato, and M. I. Kolobov, Phys. Rev. Lett. **83**, 1763 (1999).

[22] V. Giovannetti, S. Lloyd, and L. Maccone, Science **306**, 1330 (2004); P. M. Anisimov, G. M. Raterman, A. Chiruvelli, W. N. Plick, S. D. Huver, H. Lee, and J. P. Dowling, Phys. Rev. Lett. **104**, 103602 (2010).

[23] F. Hudelist, J. Kong, C. Liu, J. Jing, Z. Y. Ou, and W. Zhang, Nature Comm. **5**, 3049 (2014)

[24] T. Sh. Iskhakov, A. M. Pérez, K. Yu. Spasibko, M. V. Chekhova, and G. Leuchs, Opt. Lett. **37**, 1919 (2012).

[25] C. K. Law and J. H. Eberly, Phys. Rev. Lett. **92**, 127903 (2004).

[26] M. V. Fedorov, Y. M. Mikhailova, and P. A. Volkov, J. Phys. B: At. Mol. Opt. Phys. **42**, 175503 (2009).

[27] A. Christ, B. Brecht, W. Mauerer, and C. Silberhorn, New J. Phys. **15**, 053038 (2013).

[28] A. Eckstein, B. Brecht, and C. Silberhorn, Opt. Express **19**, 13770 (2011).

[29] P. Sharapova, A. M. Pérez, O. V. Tikhonova, and M. V. Chekhova, Phys. Rev. A **91**, 043816 (2015).

[30] F. M. Miatto, H. di Lorenzo Pires, S. M. Barnett, and M. P. van Exter, Eur. Phys. J. D **66**, 263 (2012).

[31] D. N. Klyshko, JETP **77**, 222 (1993).

[32] A. Pérez, A. Cavanna, F. Just, M. V. Chekhova, and G. Leuchs, Laser Phys. Lett. **10**, 125201 (2013).

[33] A. Cavanna, A. M. Pérez, F. Just, M. V. Chekhova, and G. Leuchs, Opt. Express **22**, 9983 (2014).

[34] A. M. Pérez, T. Sh. Iskhakov, P. Sharapova, S. Lemieux, O. V. Tikhonova, M. V. Chekhova, and G. Leuchs, Opt. Lett. **39**, 2403 (2014).

[35] A. Meda, S. Olivares, I. P. Degiovanni, G. Brida, M. Genovese, and M. G. A. Paris, Opt. Lett. **38**, 3099 (2013).

[36] G. Brida, I. P. Degiovanni, M. Genovese, A. Meda, S. Olivares, and M. Paris, Phys. Scr. T **153**, 014006 (2013).

[37] D. V. Reddy, M. G. Raymer, and C. J. McKinstrie, Opt. Lett. **39**, 2924 (2014).

[38] B. Brecht, A. Eckstein, R. Ricken, V. Quiring, H. Suche, L. Sansoni, and C. Silberhorn, Phys. Rev. A **90**, 030302 (2014).